Indian Journal of Geo Marine Sciences
Vol. 50 (06), June 2021, pp. 445-453

Assessment of tidal current energy in Bohai Sea and Yellow Sea, China

S Yuan[a], P Yuan*[,a,b], X Si[a,b], X Liu[a], J Tan[a,b] & S Wang[a,b]
[a]Ocean University Of China, Tsingtao – 266 100, China
[b]Ocean Engineering Key Laboratory of Tsingtao, Qingdao – 266 100, China
*[Email: yuanpeng50@hotmail.com]

Received 02 April 2019; revised 28 October 2019

In china, Bohai Sea and Yellow Sea are major shallow water areas. There are many regions with high current velocities which are potential sites for tidal energy development. In this paper, a 3D numerical model, verified by the measured data, was built to quantify the extractable current energy along the coast of the Bohai Sea and Yellow Sea. By using tidal harmonic analysis method, 4 major constituents' harmonic constants and ellipse parameters, including M_2, S_2, K_1, O_1, were calculated. The tidal currents' characteristics in Bohai Sea and Yellow Sea were analyzed and their maximum probable velocity could be obtained. The FLUX method was applied to calculate the kinetic energy flux through the front cross-sectional area of the flow channel. Based on numerical simulation results, the tidal current energy in three regions, including Shandong Peninsula, Bohai Strait and Liaodong Bay, was evaluated. The results showed that the maximum tidal current energy density, 6.2 kW/m^2 and 5.5 kW/m^2, might occur at mid-ebb in the east of Shandong Peninsula and in the northeast of Bohai Strait, respectively. In addition, Tidal Stream Exploitability (TSE) method was used to find optimal areas of tidal farm in Chengshan Cape. The detailed results about power density distribution in Bohai Sea and Yellow Sea would be given by further analysis.

[**Keywords**: Bohai Sea, Current, Numerical model, Tidal energy, Yellow Sea]

Introduction

In response to the crisis caused by global climate change and fossil-fuel energy pollution, extracting power from ocean draws increasing attention. The tidal current energy, which is regarded as carbon-free renewable energy, has advantages of predictability and relatively less environmental interference[1,2]. In recent years, extracting tidal current energy has become the focus of research in coastal countries such as the United Kingdom[3], the United States[4], and Canada[5].

Generally, two approaches can be applied to calculate the amount of tidal current energy resources, including extensively current measurement and numerical modelling[6]. Nowadays, most research focus on far-field fluid dynamics. One-dimensional (1D), two-dimensional (2D), and three-dimensional (3D) numerical models of hydrodynamics have been employed[7]. Blunden *et al.*[8] applied a 2D tidal-driven hydrodynamic model to analysis the available tidal current energy resources at Portland Bill, UK. Sena *et al.*[9] developed a 2D depth-averaged shallow water model of the natural tidal dynamics in the southwestern UK and Irish Sea to assess the extractable power; Wang *et al.*[10] studied the possibility of obtaining tidal energy from Agate Pass and Rich Passage, meanwhile they used the 3D model FVCOM with an embedded MHK module to quantify the power production rates; Scott *et al.*[11] applied DG-ADCIRC to build a numerical model for estimating the maximum power. Their results showed that the tidal energy could be extracted by placing tidal stream power devices on the Pentland Firth and/or the individual sub-channels formed by Swona, Stroma and the Pentland Skerries islands.

The tidal current energy resource in china is abundant along Bohai Sea's and Yellow Sea's offshore waters[12]. There are long coastlines and many of the high velocity sites are suitable for energy extraction[13,14]. In order to find waters with greatest potential and to evaluate the tidal energy production, a 3D hydrodynamic numerical model of Bohai Sea and Yellow Sea, verified with measured data, was built by FVCOM. This model could predict the changes of the tidal current both in space and time, thus it would become a useful tool for evaluating tidal current energy resources. The remainder of the paper is presented as follows. First, the numerical simulation of tidal flow, model setting and the method of tidal current energy extraction were presented followed by validation of the model results. Next, the

hydrodynamics and physical characteristics of the tidal current characteristics in Bohai Sea and Yellow Sea were analyzed. The following section dealt with the distribution of probable maximum velocity using harmonic analysis method. Third, high tidal velocities could be found in several locations in Bohai Sea and Yellow Sea, notably around Shandong Peninsula, Bohai Strait and Liaodong Bay. The corresponding power energy density in these regions was computed. Finally, Tidal Stream Exploitability (TSE) method was used to find optimal areas of tidal farm in Chengshan Cape.

Materials and Methods

In this work, the unstructured-grid, finite-volume, coastal ocean model (FVCOM)[15] was used to simulate. FVCOM controls the flux between volumes by calculating non-overlapping horizontal triangles, and simulates water surface elevation, velocity, salinity, temperature, sediment, and other scalar components in an integral form. By adopting unstructured triangular elements in horizontal plane and the sigma stretch coordinate system in vertical direction, the model is particularly suitable for representing complex coastlines and bottom topography[10].

The main governing equations in this paper are given as:

$$\frac{\partial u}{\partial t}+u\frac{\partial u}{\partial x}+v\frac{\partial u}{\partial y}+w\frac{\partial u}{\partial z}-fv=$$
$$-\frac{1}{\rho_o}\frac{\partial(p_H+p_a)}{\partial x}-\frac{1}{\rho_o}\frac{\partial q}{\partial x}+\frac{\partial}{\partial z}(K_m\frac{\partial u}{\partial z})+F_u \quad \ldots (1)$$

$$\frac{\partial v}{\partial t}+u\frac{\partial v}{\partial x}+v\frac{\partial v}{\partial y}+w\frac{\partial v}{\partial z}+fu=$$
$$-\frac{1}{\rho_o}\frac{\partial(p_H+p_a)}{\partial y}-\frac{1}{\rho_o}\frac{\partial q}{\partial y}+\frac{\partial}{\partial z}(K_m\frac{\partial u}{\partial z})+F_v \quad \ldots (2)$$

$$\frac{\partial P}{\partial z}=-\rho g \quad \ldots (3)$$

$$\frac{\partial w}{\partial x}+\frac{\partial w}{\partial y}+\frac{\partial w}{\partial z}=0 \quad \ldots (4)$$

$$\frac{\partial T}{\partial t}+u\frac{\partial T}{\partial x}+v\frac{\partial T}{\partial y}+w\frac{\partial T}{\partial z}=\frac{\partial}{\partial z}(K_h\frac{\partial T}{\partial z})+F_T \quad \ldots (5)$$

$$\frac{\partial S}{\partial t}+u\frac{\partial S}{\partial x}+v\frac{\partial S}{\partial y}+w\frac{\partial S}{\partial z}=\frac{\partial}{\partial z}(K_h\frac{\partial S}{\partial z})+F_S \quad \ldots (6)$$

$$\rho=\rho(T,S) \quad \ldots (7)$$

where, x, y and z stand for east, north, and vertical axes in the Cartesian coordinate system; u, v and w represent velocity components of x, y, z; T, S, ρ and P are water's temperature, salinity, density and pressure, respectively; f and g are the Coriolis parameter and the gravitational acceleration; K_m is the vertical eddy viscosity coefficient; and K_h is the thermal vertical eddy diffusion coefficient. F_u, F_v, F_T, and F_S represent the horizontal momentum, thermal and salt diffusion terms.

Furthermore, the drag coefficient C_d is influenced by matching a logarithmic bottom layer to the model at a height Z_{ab} above the bottom. The C_d formula is given as:

$$C_{\mathrm{d}}=\max(k^2/\ln(\frac{z_{ab}}{z_o}),0.0025) \quad \ldots (8)$$

where, k is the von Karman constant and this value equals 0.4; Z_{ab} represents the bottom roughness parameter.

The methods of tidal current energy extraction have developed rapidly in the recent years. Chen *et al.*[16] reported that they used the momentum sink method to calculate the tidal current energy in Zhaitang Island. Neill *et al.*[17] conducted a model to estimate tidal resource between the island of Alderney and the Cap de la Hague. In this study, the turbine array was represented by an additional bed roughness term in the control flow equations. Draper *et al.*[18] and Adcock *et al.*[19] studied the power distribution of the idealized headland, and regarded the influence of turbine arrays as line sinks of momentum, which was related to the Linear Momentum Actuator Disk Theory. These above studies incorporate the tidal device into ocean model to evaluate the extraction of tidal energy. Furthermore, in term of Tidal Assessment System[20] which was published by European Ocean Energy Center (EMEC) in 2009, Flux method was also widely used to estimate tidal current energy. Liang *et al.*[21] and Jiang *et al.*[22] used this way to assess Shandong Peninsula's and Zhaitang Island's tidal energy resource in China, respectively. In present work, the tidal current energy resource was estimated by Flux method. The kinetic power density from the tidal current can be given as:

$$P=\frac{1}{2}\cdot\rho\cdot V^3 \quad \ldots (9)$$

$$P_m=\frac{1}{2}\cdot\rho\cdot\overline{V}^3 \quad \ldots (10)$$

Where, V and $\overline{V}$ are the tidal current velocity and the average tidal current velocity, respectively.

Flux:

$$P_{Flux} = P_m \cdot A \quad \ldots (11)$$

$$P_{Flux} = P \cdot A \quad \ldots (12)$$

$$P_{Available} = P_{Flux} \cdot SIF \quad \ldots (13)$$

where, P_{Flux} stands for total energy resources; P_m represents the average tidal current power density; A is cross-section area of the channel; *SIF* is an important impart factor which represents the percentage of the total tidal energy resource that can be extracted with small economic or environment effects. The values of *SIF* which refer to article[23] are 20 %, 15 % and 10 %. In this paper, SIF was defined as 20 %.

An unstructured computational mesh was used for the domain and this covered the region 35.5 °N ~ 41° N and 117.5° E ~ 127° E (Fig. 1). Five sigma layers were set to get the structure of tidal flows in vertical direction. The model's open boundary was forced by sea surface elevation consisting of eight dominant constituents (M_2, S_2, N_2, K_2, K_1, O_1, P_1, Q_1), which were obtained from the global tidal model TPXO7.2. The river inflows, density-induced as well as wind-driven circulation were not considered because this work mainly focused on barotropic tidal circulation, and the salinity and temperature of this model were set as constants: 32 and 20 °C, respectively.

Results and Discussion

The verification data was obtained from the Tide Tables[24] for ensuring the accuracy of tidal elevations' results at different sites, whose locations are showed in Table 1. The model started running for 35 days since 27/05/2013. As spin-up period was essential to make the initial conditions have small effects on the numerical results during the validation period. Finally, 3 days was selected as a spin-up period for all simulations. The comparisons of the modeled tidal elevations and available elevations at tide gauges are showed in Figure S1. It can be seen that there is a good agreement between the simulated results and the observations no matter in amplitude or phase. The RMSE (root-mean-square error) of tidal elevations over these gauges are 0.27 m, 0.13 m, 0.14 m, and 0.16 m, respectively.

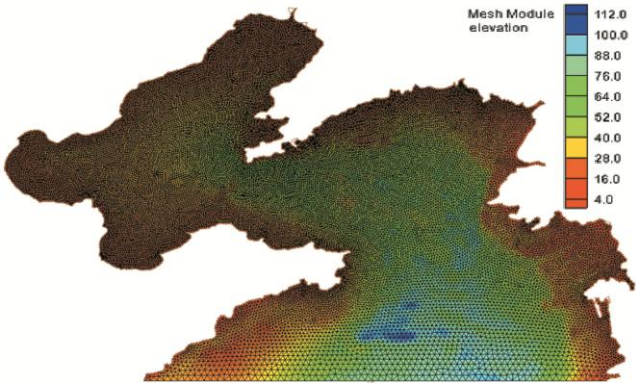

Fig. 1 — Computing grid distribution in Bohai Sea and the northern part of the Yellow Sea

In addition, the measured current velocities obtained at two sites which are listed in Table 2 were compared with the model's results. The tidal currents at different layers were validated. Owing to lack of the measured current data of 2013, the model, however, was run for 3 days since 8/12/2010 and the spin-up period for all simulations was set as 1 day. The time series comparisons of current velocity are plotted in Figures S2 & S3. The RMSE of velocities at different layers are presented in Table 3. It can be seen that the current predictions are close to measured data.

The model results provided a sufficiently long time series for harmonic analysis with four main components (M_2, S_2, K_1, O_1). Table S1 shows the comparisons between observed harmonic constituents which are obtained at 20 gauging stations (Fig. S4) and the model's M_2, S_2, K_1 and O_1 constituents for tidal elevations. The results show that the average absolute deviations in amplitude of these constituents are 4.57 cm, 4.62 cm, 3.84 cm, and 4.86 cm, respectively, and those of phase are 6.78°, 4.6°, 3.81°, and 6.02°, respectively. Analysis of the harmonics reveals that a close agreement is found between the simulated results and observations, and their errors are within acceptable ranges.

Table 1 — Coordinate of measurement point

Measurement point	Longitude (E)	Latitude (N)
Bayuquan	122.08°	40.30°
Dalian	121.68°	38.87°
Yantai	121.38°	37.55°
Tsingtao	120.30°	36.08°

Table 2 — Coordinate of measurement point

Measurement point	Longitude (E)	Latitude (N)	Depth (m)
No. 1 site	122°42.56'	37°23.75'	30
No. 2 site	122°43.06'	37°23.74'	50

Table 3 — Error analysis

Layer RMSE (m/s) Site	No. 1 site	No. 2 site
Shallow layer	0.1	0.27
Middle layer	0.13	0.28
Bottom layer	0.14	0.26

Figure 2 plots the results of the surface tidal current ellipses of M_2, S_2, K_1 and O_1. The ellipse charts provide the magnitudes of the tidal currents by using major and minor axes to represent maximum and minimum velocities, respectively. The pattern of semi-diurnal ellipse shows similar characteristic in Bohai Sea and Yellow Sea, while the M_2 tidal current's value is bigger than that of S_2. The M_2 semi-diurnal currents are high on east coast of Shandong Peninsula and on west coast of Korea, and their maximum values are over 1.5 m/s. Furthermore, the distribution of K_1 tidal current is similar to that of O_1 in study waters. Figure 2 shows that the strong K_1 diurnal currents occur in the Bohai Strait and Liaodong Bay where maximum velocity could reach 0.4 m/s.

When evaluating the energy of the power flow, the current speed is very important, because the power of the power flow will change with the cube of its velocity. According to paper by De *et al.*[25], the maximum probable velocity can be estimated as the large values given by equations:

$$V_{\max} = 1.29W_{M_2} + 1.23W_{S_2} + W_{K_1} + W_{O_1} \quad \ldots (14)$$

$$V_{\max} = W_{M_2} + W_{S_2} + 1.68W_{K_1} + 1.46W_{O_1} \quad \ldots (15)$$

Where, W is the length of the major axis of the respective components.

The distribution of maximum probable current velocity in Bohai Sea and Yellow Sea is shown in Figures 3. The strong currents occur in Shandong Peninsula, the Bohai Strait and the Liaodong Bay. The strongest currents are found at the eastern cape of Shandong Peninsula (where named Chengshan Cap) and in the north of the Bohai Strait (where named Laotieshan channel), where the current velocity could both exceed 2 m/s. According to measured current data which had been published, the flow velocities were over 2.3 m/s 26 in Chengshan Cap and those were about 1.8 m/s 27 in Laotieshan channel. These above measured data verified the waters where we had chosen accurately. Furthermore, the strongest current is on order of 1.5 m/s in the Liaodong Bay. Also accounting for regional planning and offshore

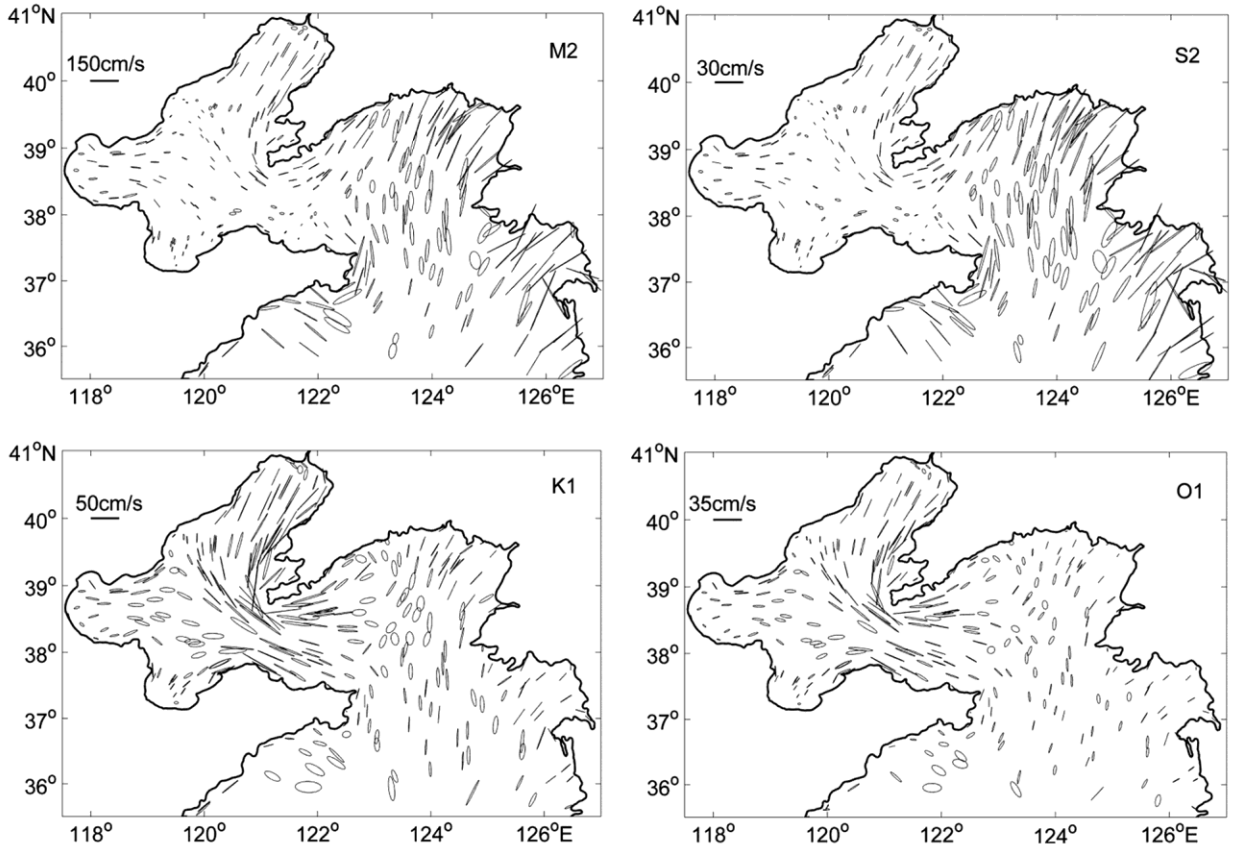

Fig. 2 — The results of tidal current ellipse

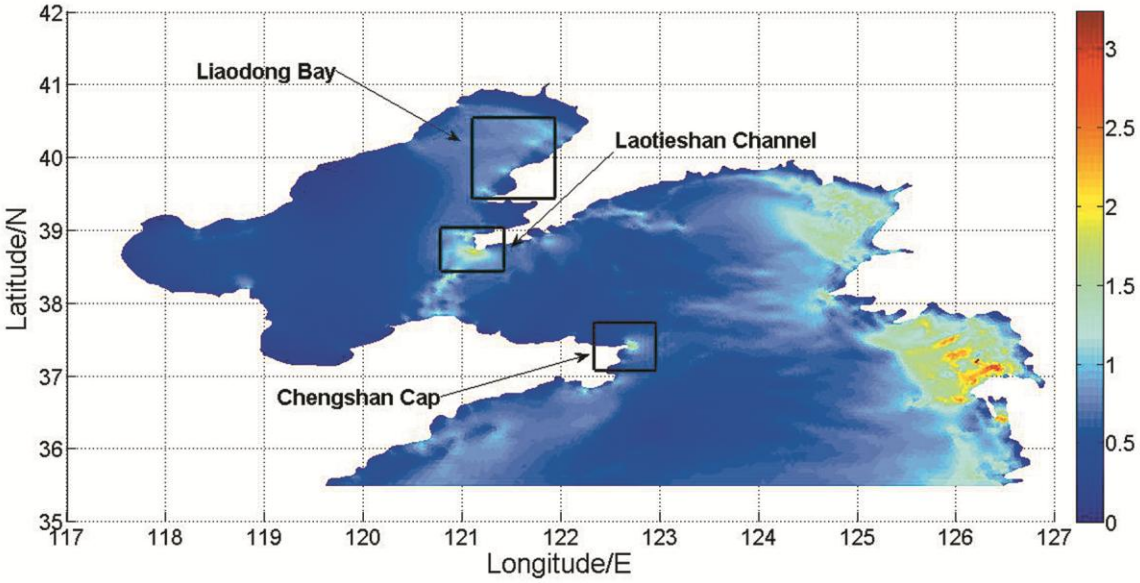

Fig. 3 — The distribution of maximum probable velocity in Baohai Sea and Yellow Sea

distance, these three regions were potential sites for tidal current energy exploitation.

The distribution of maximum (Fig. 4a) and mean (Fig. 4b) tidal current velocity within 30 days surrounding Shandong Peninsula reveal some differences in the model results. Generally, maximum velocities are under 1 m/s, mainly associated with flow around Chengshan Cap, where the current exceed 2.0 m/s. The maximum mean velocities occurring in Chengshan Cape are also much higher than other water areas, and those could reach 1m/s at the peak ebb.

The power density in this work is calculated to choose the locations with abundant tidal current energy. In previous studies, various mean power density thresholds were employed in Chengshan Cape to determine promising tidal energy extraction locations. These included 0.93 kW/m^2[ref. 13], 1.1 kW/m^2[ref. 26]. In this paper, the distribution of maximum and mean power density (Fig. 5) are got by using Equations (8) and (9). The magnitudes of maximum power density are generally smaller than 1 kW/m^2 for study waters, and high values primarily occur in Chengshan Cape where the largest value is about 6.3 kW/m^2. By contrast, the maximum value of mean power density is about 0.5 kW/m^2.

Based on the model-computed mean power density and the cross-section area of channel that can be defined as 80500 m^2 referring to article 28, Equations (11) and (13) gave an estimated total and available

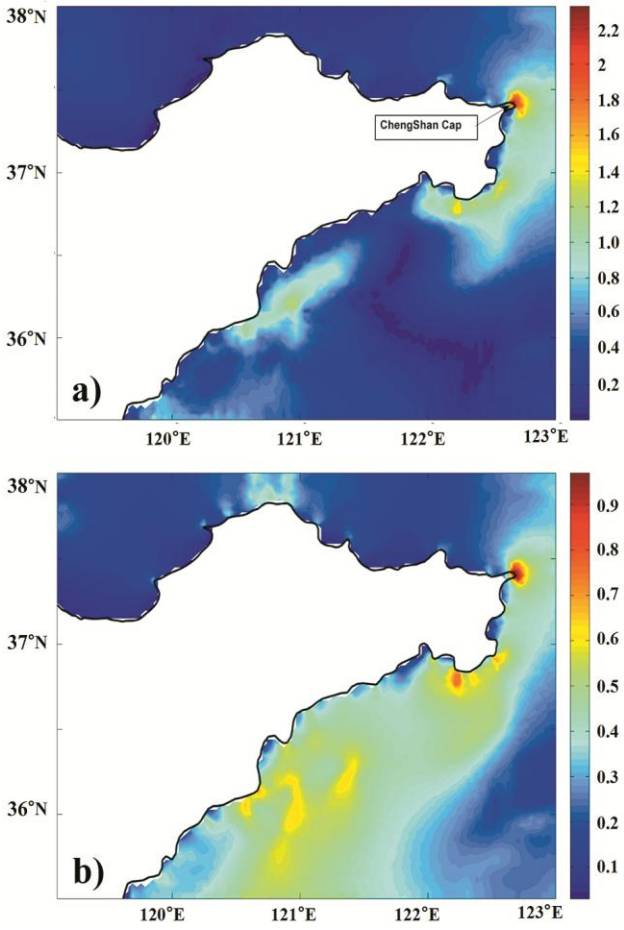

Fig. 4 — The distribution of maximum velocity (a), and mean velocity (b)

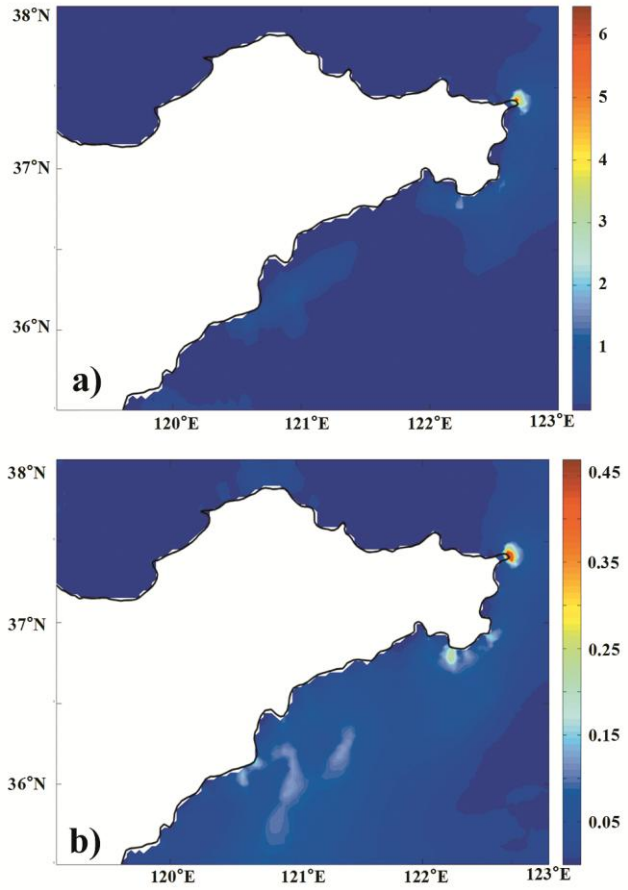

Fig. 5 — The distribution of maximum power density (a), and mean power density (b)

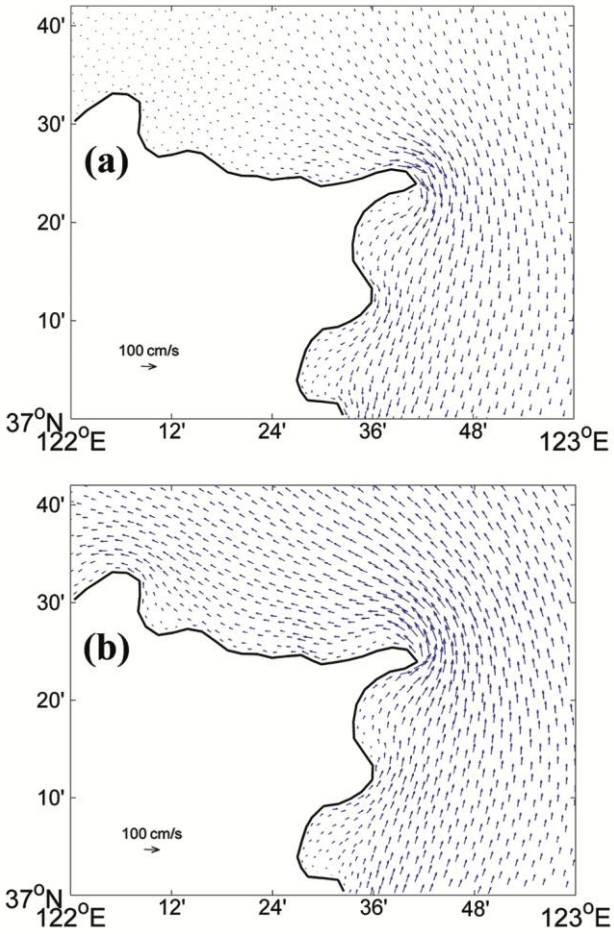

Fig. 6 — Mid-flood (a), and mid-ebb (b) tidal flow field of Chenshan Cap

tidal current energy in Chengshan Cape of 40.3 MW and 8.1 MW, respectively.

The mid-flood and mid-ebb flow patterns of Chengshan Cape are presented in Figure 6. A tidal asymmetry of velocities is apparent: during the flood, the tidal wave propagates southward, and the peak velocity can reach 2.3 m/s. While during the ebb, the tidal wave propagates southward, and the velocity can reach 1.9 m/s. The tidal asymmetry may be induced by changes in the geometry of the region at different tidal levels[29].

The site with the largest mean power density (Fig. 7), with a peak value of 0.8 kW/m^2, is Laotieshan channel. The water depth over this patch, which is marked on NoAA charts, ranges from 50 to 60 m, and is suitable for turbine emplacement. In the eastern part of Liaodong Bay, the maximum mean power density (Fig. 8), which is higher than other waters areas is about 0.7 kW/m^2.

Figure 9 plots the variation of instantaneous power density time series during 30-day simulation period.

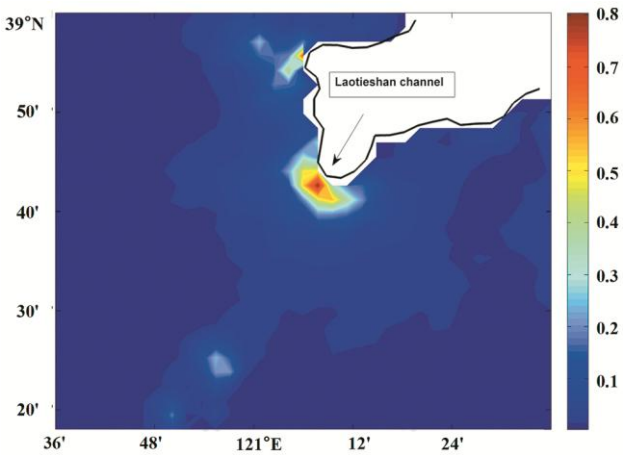

Fig. 7 — The distribution of mean power density in Laotieshan channel

The power density time series show intense temporal variations in spring and neap tidal cycles. The power density during spring tides is nearly an order of magnitude greater than during neap tides; the reason of

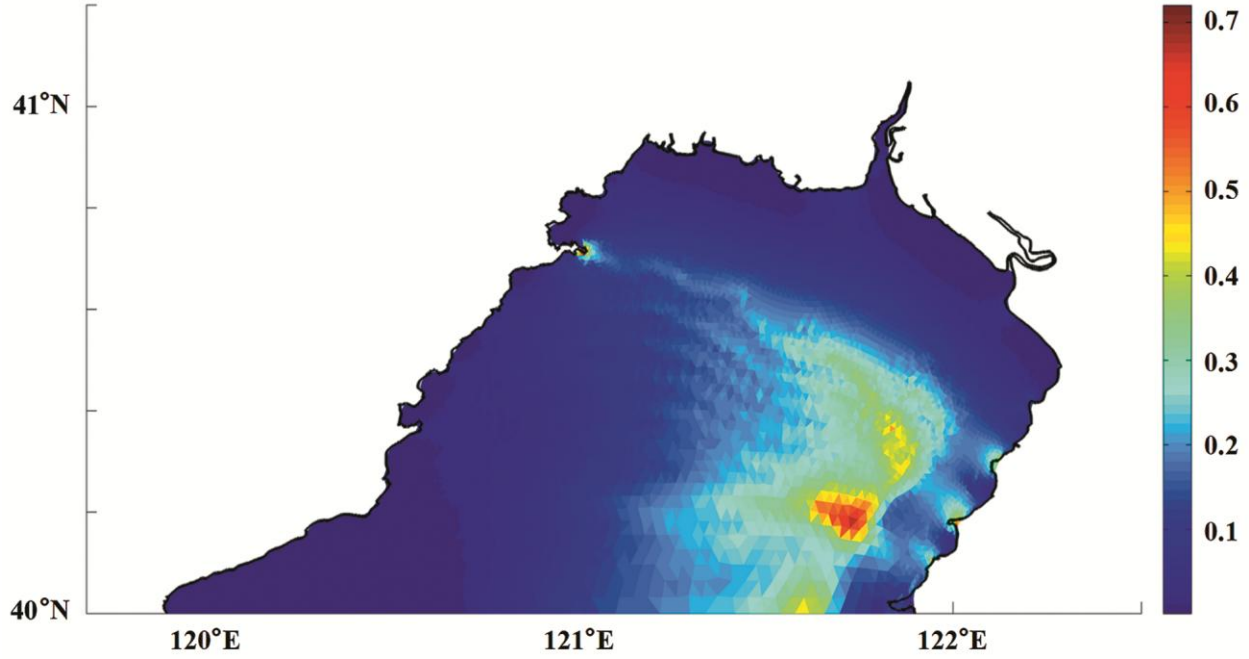

Fig. 8 — The distribution of mean power density in Liaodong Bay

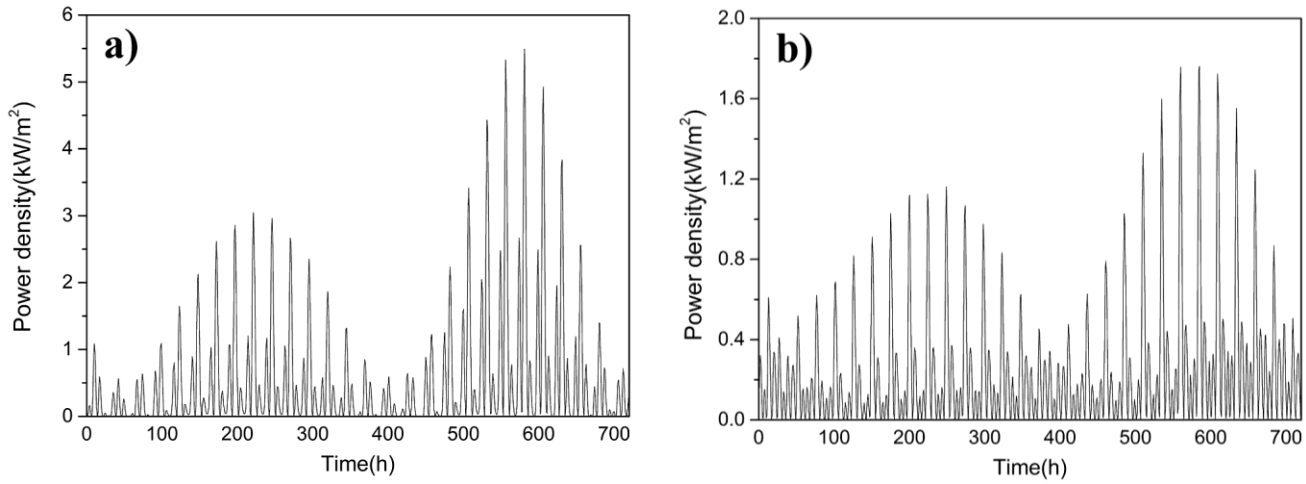

Fig. 9 — Instantaneous power density of maximum velocity grid in Laotieshan channel (a), and Liaodong Bay (b)

this is that the power density is proportional to the cube of tidal current velocity. The maximum instantaneous power density calculated with Equation (8) reaches approximately 5.5 kW/m^2 and 1.7 kW/m^2 in Laotieshan channel and Liaodong Bay, respectively.

In many waters, strong currents can appear with limited water depth, so more attention must be paid to water depth in the analysis. In this work, Tidal Stream Exploitability (TSE) index, which was proposed by Iglesias[29], is used to find optimal areas to place tidal devices. It is based on the available power per unit width of the tidal current, which is determined by combining the possible tidal asymmetry at the maximum speed during flood and ebb tides[30]. The Equation for estimating the TSE index is given as:

$$TSE = \frac{\xi}{2V_0^3 h_0}(V_f^3 + V_e^3)h \quad \ldots (16)$$

where, V_0 and h_0 stand for characteristic velocity and characteristic water depth, respectively. The interest of these characteristic magnitude lies in its dimensions rather than their numeric values, which only reflect the magnitude of each variable; V_f and V_e represent the depth-mean velocities at mid-flood and

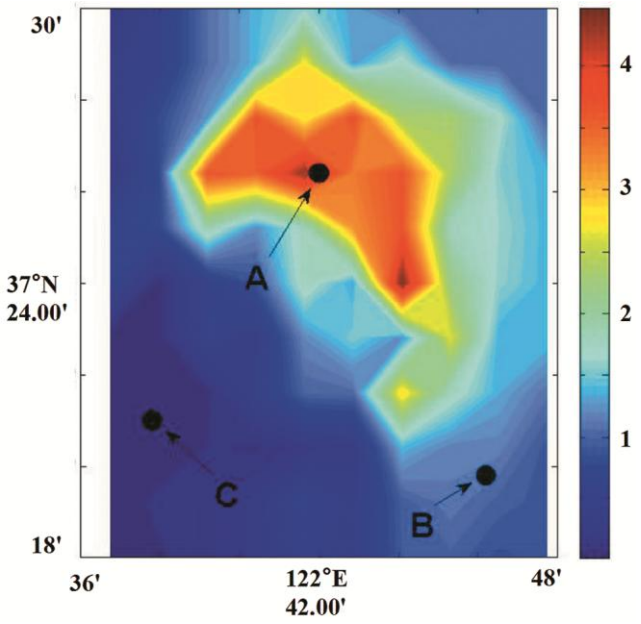

Fig. 10 — The TSE index distribution

mid-ebb tides, respectively; and h is the water depth; ξ is the penalty function of the tidal current energy, it can be written as:

$$\xi = 0 \quad if \quad h - \frac{\Delta h}{2} \le h_1$$

$$\xi = \frac{1}{h_2 - h_1}(h - \frac{\Delta h}{2} - h_1) \quad if \quad h_1 < h - \frac{\Delta h}{2} < h_2,$$

$$\xi = 1 \quad if \quad h - \frac{\Delta h}{2} \ge h_2$$

where, Δh is the maximum tidal range, and h_1 and h_2 are the lower and upper limits of the penalty range, respectively.

As shown in Figure 4, the surrounding waters of Chengshan Cape (37.3° N ~ 37.5° N, 122.6° E ~ 122.8° E) are chosen to calculate the distribution of TSE index and several areas marked as A (37.43° N, 122.7° E), B (37.33° N, 122.77° E) and C (37.35° N, 122.62° E) in this region are selected for tidal current farm. In this paper, the values are V_0 = 1.0 m/s and h_0 = 26.66 m.

The TSE index was calculated in terms of Equation (15). Figure 10 indicates that the quality of tidal energy resources in most areas is below the reference value. However, near the area A, the quality of tidal current energy is about 4.5 to 5 times the reference value. Area A has a water depth of more than 32 m and is a potential place to develop tidal energy. By contrast, due to the weak flow (Table 4), area B is not suitable for the tidal power station in the

Table 4 — The basic data of areas A, B and C

	Depth (m)	Maximum tidal current velocity (m/s)	TSE
A	32.3	1.89	4.3
B	37.85	0.82	0.4
C	5.78	1.57	1.1

TSE graph. On the other hand, area C (Table 4) shows the opposite situation: strong flow, but insufficient water depth.

In summary, the TSE index used in this work is based on water depth and flow information. Where the water depth is sufficient but the flow is weak or the flow is large but the water depth is insufficient, showing low TSE values.

Conclusion

In this paper, a 3D numerical ocean model was built up and successfully validated to study the tidal waves occurring in Bohai Sea and Yellow Sea. The results showed that the velocity of M_2 tidal currents were high on the western coast of Korea, and its maximum value was about 1.5 m/s. Strong K_1 tidal currents were found in the Bohai Strait. The pattern of M_2 is similar to that of S_2. The pattern of K_1 is similar to that of O_1.

In term of the distribution of maximum probable current velocity, the waters surrounding Chengshan Cape, Laotieshan channel and the east of Liaodong Bay were potential sites for extracting tidal current energy. The greatest flow velocities for ebb tides of these three regions were about 2.3 m/s, 2.1 m/s and 1.5 m/s, respectively; and the corresponding values of power density were 6.5 kW/m^2, 5.5 kW/m^2 and 1.8 kW/m^2, respectively.

A study in Chengshan Cape has been developed to demonstrate the TSE method. Three different areas emerged in this region. Area C had a higher power density, while its TSE values were penalised by shallow water, which may cause significant restrictions on the development of tidal resources. The TSE values of area B with sufficient water depth were low due to weak flow. Only area A has potential for a tidal current farm because of its large power density and appropriate water depth.

Supplementary Data

Supplementary data associated with this article is available in the electronic form at http://nopr.niscair.res.in/jinfo/ijms/IJMS_50(06)445-453_SupplData.pdf

Acknowledgements

The study is supported by the Major Basic Research Project of Shandong Province (ZR2017ZA0202) and the National Natural Science

Foundation of China (Nos. 51779238). The authors are grateful for the financial support.

Conflict of Interest

There is no conflict of interest.

Author Contributions

SY: Numerical simulation, writing original draft, and data processing; PY: Methodology and writing original draft; XS: Validation and data processing; and JT, XL and SW: Writing—review and editing.

References

1 Yang Z Q, Wang T & Copping A E, Modeling tidal stream energy extraction and its effects on transport processes in a tidal channel and bay system using a three-dimensional coastal ocean model, *Renew Energy*, 50 (3) (2013) 605-613.

2 Copping A E, Geerlofs S H & Hanna L A, The contribution of environmental siting and permitting requirements to the cost of energy for oscillating water column wave energy devices, (Pacific Northwest National Laboratory Richland, Washington, United States), 2013. https://doi.org/10.2172/1171907

3 Neill S P, Vogler A, Goward-Brown A J, Baston S, Lewis M J, *et al*., The wave and tidal resource of Scotland, *Renew Energy*, 114 (2017) 3-17.

4 Defne Z, Haas K A & F+ritz H M, Numerical modeling of tidal currents and the effects of power extraction on estuarine hydrodynamics along the Georgia coast, USA, *Renew Energy*, 36 (12) (2011) 3461-3471.

5 Sutherland G, Foreman M & Garrett C, Tidal current energy assessment for Johnstone strait, vancouver island, *P I MechEng A-J Pow*, 221 (2) (2007) 147-157.

6 Jeyaraj S K, Balaji R & Vengatesan V, *2nd International Conference on Offshore Renewable Energy* (Core), 12 September, 2016 - 14 September, 2016, Glasgow, UK. https://books.google.co.in/books?id=BEVYAQAACAAJ

7 Work P A, Haas K A, Defne Z & Gay T, Tidal stream energy site assessment via three-dimensional model and measurements, *Appl Energy*, 102 (2013) 510-519.

8 Blunden L S & Bahaj A S, Initial evaluation of tidal stream energy resources at Portland Bill, UK, *Renew Energy*, 31 (2) (2006) 121-132.

9 Serhadlıoğlu & Sena, Tidal stream energy resource assessment of the Anglesey Skerries, *Int J Mar Energy*, 3 (2013) e98-e111.

10 Wang T P & Yang Z Q, A modeling study of tidal energy extraction and the associated impact on tidal circulation in a multi-inlet bay system of Puget Sound, *Renew Energy*, 114 (2017) 204-214.

11 Draper S, Adcock T A A, Borthwick A G L & Houlsby G T, Estimate of the tidal stream power resource of the pentland firth, *Renew Energy*, 63 (2014) 650-657.

12 Wang C K & Lu W, *Ocean energy resources analysis method and the evaluation of the reserves*, (China Ocean Press, Beijing), 2009, pp. 153.

13 He W U, Wang X & Han L S, Assessment of extractable energy of tidal current at Chengshantou cape, *Oceanol Limnol Sin*, 44 (2) (2013) 570–576.

14 Gao F, Guang L I & Qiao L L, Resource assessment of the idal energy around the shandong peninsula, *Periodical Ocean Univ China*, 42 (12) (2012) 91-96.

15 Chen C S, Liu H & Beardsley R C, An unstructured grid, Finite-Volume, three-dimensional, primitive equations ocean model: Application to coastal ocean and estuaries, *J Atmos Oceanic Technol*, 20 (20) (2003) 159-186.

16 Chen Y, Lin B, Lin J & Wang S, Effects of stream turbine array configuration on tidal current energy extraction near an island, *Comput Geo Sci*, 77 (2015) 20-28.

17 Neill Simon P, Jordan J R & Couch S J, Impact of tidal energy converter (TEC) arrays on the dynamics of head lands and banks, *Renew Energy*, 37 (1) (2012) 387-397.

18 Draper S, Borthwick A G L & Houlsby G T, Research article: energy potential of a tidal fence deployed near a coastal headland, *Philos Trans A Math Phys Eng Sci*, 371 (1985) (2013) 2-2. https://doi.org/10.1098/rsta.2012.0176

19 Adcock, Thomas A A & Draper S, Power extraction from tidal channels-Multiple tidal constituents, compound tides and overtides, *Renew Energy*, 63 (2014) 797-806.

20 Black & Consulting V, *Assessment of tidal energy resource*, (The European Marine Energy Centre Ltd, London), 2009, pp. 53.

21 Liang B C, Yang L L & Shi H D, *International Society of Offshore and Polar Engineers*, (Rhodes, Greece), 2012, pp. 173-179.

22 Jiang X, Wang S, Si X, Yuan P & Tan J, Tidal stream characteristic analysis and micro-sitting selection in sea area around Zhaitang island, *Acta Energiae Solaris Sinica*, 39 (4) (2018) 892-899.

23 Hagerman G, Polagye B, Bedard R & Previsic M, *Methodology for estimating tidal current energy resources and power production by tidal in-stream energy conversion (TISEC) devices*, (Report No. EPRI - TP - 001 NA Rev 2), Report by Electric Power Research Institute (EPRI), 2006, pp. 57. https://tethys.pnnl.gov/sites/default/files/publications/Tidal_Current_Energy_Resources_with_TISEC.pdf

24 National Marine Data and information Service, China, TIDE TABLES. 000.002(2002)28.

25 Song D H, Bao X W, Zhang S F & Zhang C H, Three-dimensional numerical simulation of tides and tidal currents in the Lianzhou Bay and adjacent areas, *Mar Sci Bull*, 31 (2012) 1-15 (in Chinese).

26 Qing J L, Liang M Z, Kei W U, Jing K L I, Zhan B L I, *et al*., Tidal stream energy assessment on chengshantou, *Trans Oceanol Limnol*, (2013).

27 He W, Shi M Z, Song Z, Xin W & Zhi Zhong M A, Preliminary assessment of tidal energy in Lao Tieshan channel, *Mar Sci Bull*, 30 (3) (2011) 310-314.

28 He W, Preliminary assessment of tidal current energy on Chengshantou area, *Ocean Technol*, 29 (3) (2010) 98-100 (in Chinese with English abstract).

29 Iglesias G, Sanchez M, Carballo R & Fernandez H, The TSE index–A new tool for selecting tidal stream sites in depth-limited regions, *Renew Energy*, 48 (7) (2012) 350-357.

30 He W, Wang X, Wang B, Bai Y & Wang P, Evaluation of tidal stream energy and its impacts on surrounding dynamics in the eastern region of Pingtan Island, China, *Chinese J Oceanol & Limnol*, 35 (6) (2017) 1-10.